

Experimental and numerical analysis of the cold forming process of automotive suspension springs

Berti Guido and Monti Manuel
University of Padua, DTG, Stradella San Nicola 3, I-36100 Vicenza (Italy),
guido.berti@unipd.it, manuel.monti@unipd.it.

Abstract

Nowadays in automotive industry great efforts are spent in achieving weight reduction of cars components. The coil springs are not exempt. For this component weight reduction can be obtained by reducing the spring wire diameter. However, to assure that springs maintain the required mechanical properties, it is necessary to adopt material with high strength.

In order to speed up the manufacturing process of coil springs, the trend is to produce them by cold forming of hardened wires. In this case the wires are subjected to the heat treatments of hardening and tempering before the coiling process. This leads to an improvement of productivity since it is not required a heat treatment after forming. However forming a high strength material already hardened and tempered is critical. The material presents low ductility and requires high forming forces. Moreover lubrication, which is more critical in cold forming, is demanded to the oxide layer present on the wire surface. The combination of such factors can lead to coil's failure during forming process.

To improve the knowledge on these phenomena, different production batches of hardened 54SiCr6 wire have been analysed, characterized in laboratory and correlated to the corresponding successes/failures recorded in the manufacturing of the springs. The process is sensitive both to the process conditions (such as friction), and to the set up of the spring making machine.

The further step of the investigation consisted in the development of a numerical model of the coiling process able to predict the possible failure during spring coiling. Ductile isotropic damage formulation has been adopted and different friction conditions, as well as different configurations of the coiling machine, have been considered and replicated by the model. The predicted results confirmed the failures recorded in the shop floor, as well as the high contribution of friction, which is strictly related to the external oxide layer, to the success/failure of the cold forming of the spring.

Keywords:

Finite element method, Lemaitre damage model, process optimization, spring forming.

1. Introduction

The first automotive coil spring was installed on the model-T (Ford) in 1910 (top speed 25 miles/hr). At that time the material of the spring was a steel with 500MPa as UTS. The development of the automotive market and the corresponding improvements of the components in the car lead to adopt today in mass production of suspension springs Silicon steels presenting an UTS around 1200MPa.

The demand of weight reduction of the whole car aimed at an effective reduction of fuel consumption forces the spring manufacturer to adopt higher strength martensitic steels in order to reduce the resisting section of the wire and for this reason the weight of the spring. The traditional approach in forming such materials is based on the hot coiling of the wire at high temperature to increase material formability and/or to reduce required forming forces; alternatively, if the cold forming process is chosen, the wire presents improved formability obtained by heat treatments before the spring is formed. In both cases the coiled spring has to be hardened and tempered to reach the target strength. Energy and time consumption due to the final heat treatment slow the production and increase manufacturing cost of the spring.

To reduce manufacturing time and spring weight cold forming can be adopted and the material is formed directly in its final condition (hardened and tempered): in this case the coiling process becomes more critical being the formability of these high-strength martensitic steel not very high. Further moving in the direction of much more high strength (between 1800 and 2100MPa) the cold forming of the wire can be extremely difficult leading to the failure of the coiled wire caused by the breakage of the spring [1 – 3].

Some breakages in the coiling process of such high strength steels stimulate the investigation both experimental and numerical, aimed at the determination of the causes of the material failure.

The forming forces required in the coiling of the wire increase with the high strength of the material causing the feeding force to be also increased: the feeding rolls should provide enough force to avoid the slip of the wire between the rolls. For this reason the friction between the wire and the feeding rolls should be at high level in order to provide enough tangential forces to avoid any slip of the wire. On the other hand, high friction increases the required forming force due to the higher contribution of friction forces developing in the

stationary dies: the guiding plate, the bending die and the bar controlling the axial pitch of the spring. The contribution of bending die can be reduced adopting two bending rolls where the sliding friction is substituted by a prevalent rolling friction. This solution has been successfully adopted by the spring manufacturers, which still face the problem of friction in the remaining components of the coiling machine: in the feeding system should be high and elsewhere should be low. The insertion of a lubricating station between feeding and forming should solve the problem, but it can be difficult in the industrial application as it generates a dirty area of the press and requires a cleaning step after the coiling to remove the residuals of the lubricant from the spring external surface. For these reasons the spring manufacturer asks for a wire with an external oxide which should act as a thin solid lubricant layer. If this layer is too thin it can be broken when the wire is passing between the feeding roll, causing a possible slip of the wire and an increase of friction in the forming part of the press. Slipping in the feeding rolls can be eliminated by increasing the radial pressure of the rolls on the wire, but this action can introduce a damage of the wire and finally can lead to the failure in the coiling of the spring.

For these reasons the investigation has been focused on the effect of friction, as well as on the setup of the coiling machine and is based on a preliminary experimental analysis of different wires followed by the development of a finite element model of the process able to predict the failure of wire during coiling.

Different samples of the same steels with different oxide layer have been tested in the coiling machine: most of them allow the correct manufacture of the spring, but someone resulted in the breakage of the spring during coiling. The samples have been characterized as concerns the thickness of the oxide layer and its visible morphology. Afterwards a numerical model of the spring coiling process has been developed introducing the description of Lemaitre damage model in the material properties. Relative damage has been used as the index to estimate the risk of failure when different friction and process parameters were used.

2. The industrial case

A wire of strain hardened martensitic steel (UTS = 1800MPa) has to be cold formed in a helicoidal spring presenting a variable diameter of the coils as well different axial pitches. The diameter of wire is 14.5mm, the internal diameter of the coil is varying between 85mm and 60mm and the axial pitch is varying too between 55mm and 32mm (Figure 1).

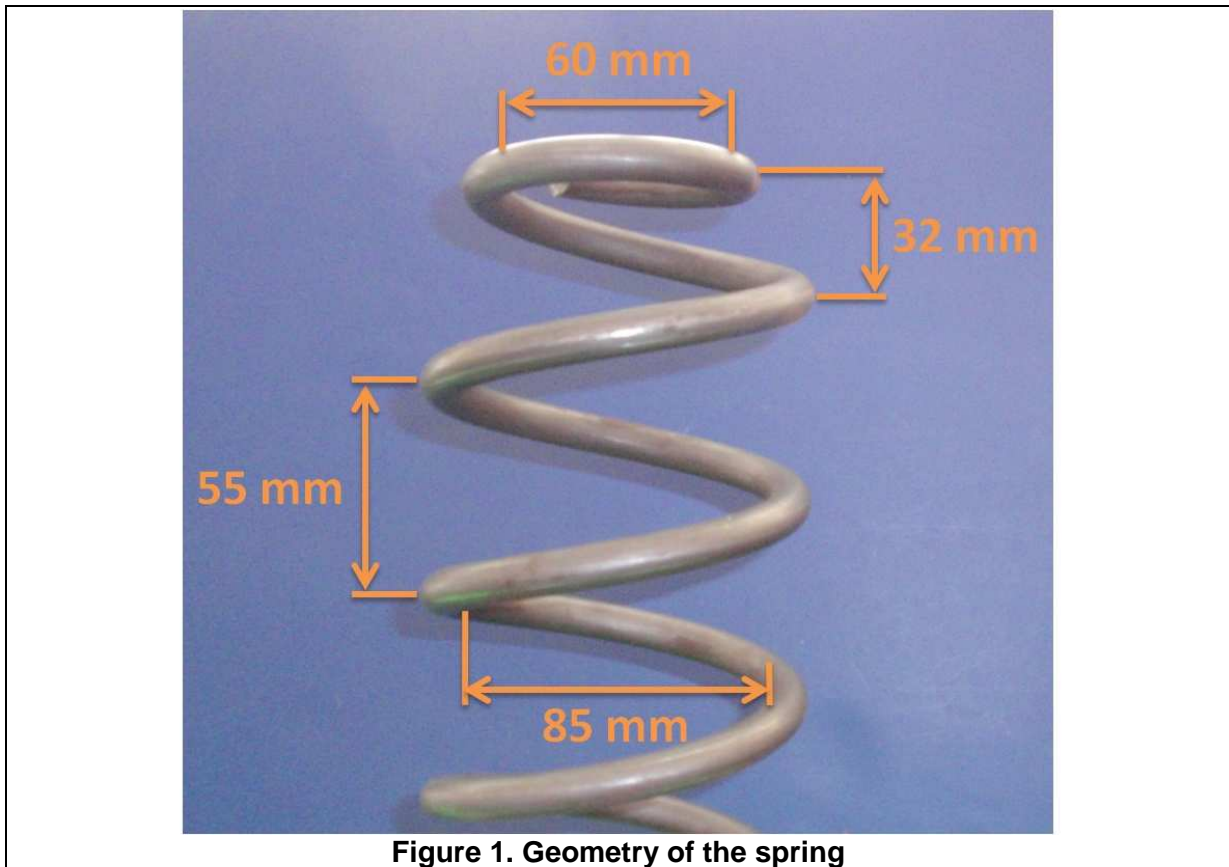


Figure 1. Geometry of the spring

The forming cycle consists in 6s and the formed spring requires a simple setting stage without further heat treatments. The spring forming machine is a Wafios numerical programmed system (Figure 2) equipped with forming rolls and a movable pitch bar which are controlled by programs and servo systems. The adoption of two forming rolls allows to reduce the friction between the wire and the forming tools and therefore the required forming force is reduced too.

The feeding rolls push the wire through the stationary guide to the forming rolls at a speed of 670mm/s and the pitch bar controls the axial pitch of the spring between 55mm (coil diameter 85mm) and 32mm (coil diameter 60mm).

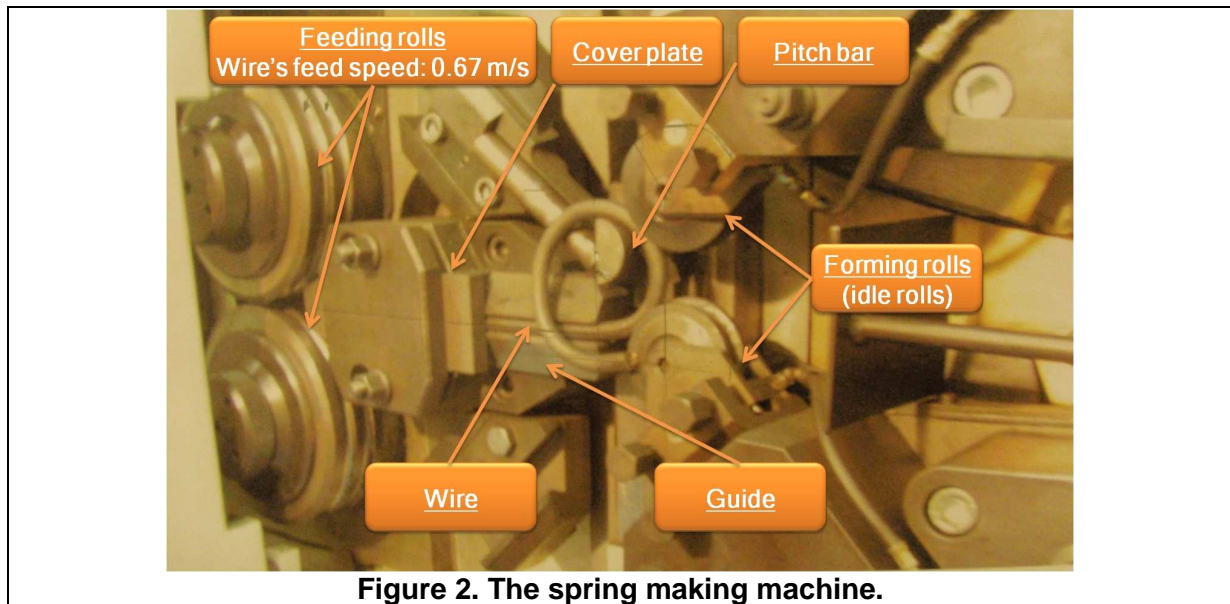


Figure 2. The spring making machine.

The spring material consists of a high-strength martensitic steel (54SiCr6) showing an UTS between 1800MPa and 1900MPa and as concerns inclusions or cracks it is defect free. This wire has been produced by cold drawing followed by a heat treatment of hardening and tempering in order to obtain the prescribed UTS, as well as a compact oxidized surface (commercially known as “black oxide”, where Fe_2O_3 is prevalent) which should act as solid lubricant during the forming of the spring. No further treatments are required before and after coiling.

During the production of the spring the spring manufacturer experienced some breakages during the coiling phase adopting almost the same setup of the coiling machine (small adjustments were performed on the shop floor as concerns the pressure applied by the feeding rolls on the wire and the position of the stationary guide), changing the wire production batch. The failure consisted in a crack on the external surface of the coil which “instantaneously” grew to a complete fracture of the coil, as shown in Figure 3.



Figure 3. The cracked coiled springs.

Different production batches of the wire to be coiled have been analysed in laboratory as concerns:

Mechanical properties (tensile test on a 8.01mm diameter specimen): the different batches present almost the same values for UTS ($1830\text{MPa} \pm 35\text{MPa}$), Young modulus ($191500\text{-}193000\text{MPa}$), Yield strength ($1620\text{-}1680\text{MPa}$), diameter after rupture ($5.3\text{-}5.5\text{mm}$). Vickers microhardness tests (load of 100g) were performed on the cross section of the drawn wires. The measurements (reported in Table 1) indicate that all wires have almost the same hardness ($650 - 680\text{HV}$).

Microstructure analysis The grain structure of the cross section of the drawn wires is almost the same for the different samples: the typical homogeneous microstructure of a tempered martensite can be recognized, as shown in Figure 4.

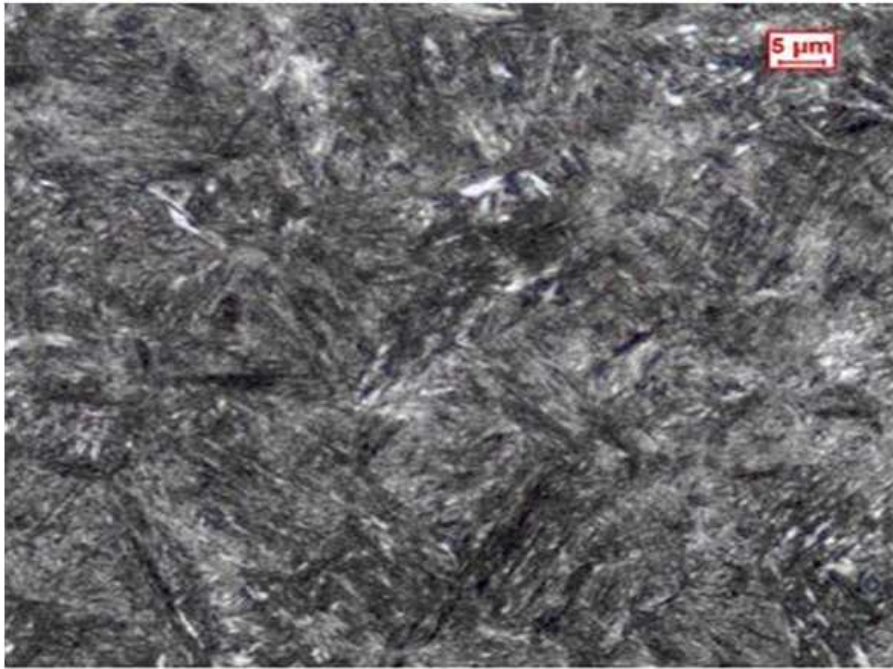


Figure 4. Micrograph of the wire.

Microscope image analysis The analysis of microscope images evidenced differences in the thickness of the oxide layer. Table 1 summarizes the optical micrographs of oxide layer and relevant measurements.

Oxidized surface testing (Nano Scratch test) the surface of the oxidized wires were scratched using a nano indenter applying an increasing normal force: the tangential force has been registered and the scratched surface has been observed. The wire with a small thickness of oxide layer shows a fragile behaviour of the layer which can be easily broken and removed revealing the underneath steel surface. When the oxide is above 8 microns the layer is more adherent and compact being deformed during scratch test. The optical micrographs of the oxide layer and scratch tests are shown in Table 1.


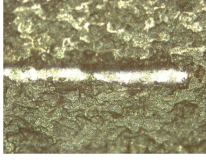
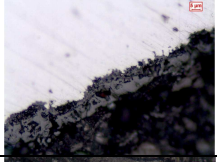
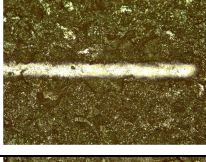
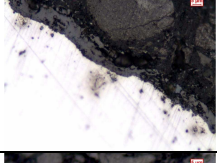
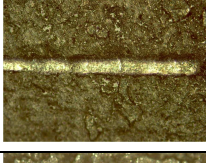
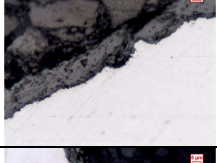
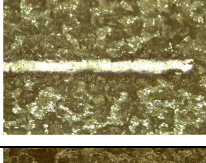
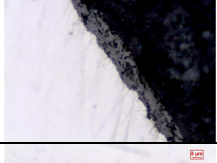
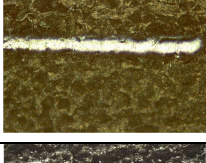
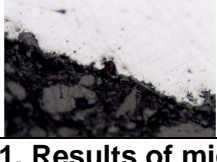
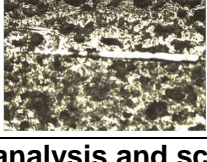
Sample	Optical micrographs of oxide layer	Optical micrographs of scratch test	Oxide thickness [μm]	Vickers Microhardness (100 g)	Formability
1			8.00	681	good
2			10.73	654	good
3			8.75	680	good
4			13.71	669	good
5			9.41	656	good
6			2.24	656	poor

Table 1. Results of microscope analysis and scratch tests relevant to different samples.

Inspection of the surface of the broken coils: near the external bending radius the surface presents a flattened area (4-5mm wide) where the oxide appears to be removed as evidenced in Figure 5.

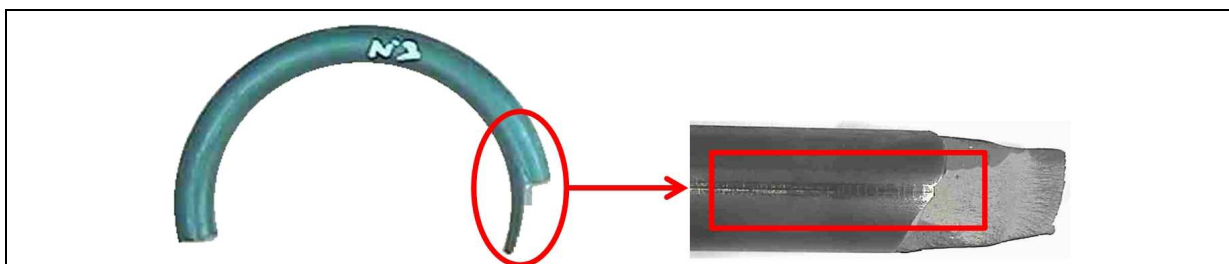


Figure 5. Detail of broken coil evidencing a flattened area where the oxide is removed.

Summarizing the results of this laboratory analysis it has been concluded that the failure of coiling process can not be directly related to

- Steel mechanical properties
- Coiling process parameters
- Configuration of forming rolls

and can be related to the oxide layer and its interaction with feeding and forming rolls.

3. Numerical modelling of the coiling process

The conclusions of the experimental analysis conducted on different production batches of the wire suggest that some interactions between the configuration of the machine, friction and the oxidized layer can cause an unacceptable level of damage during the forming process of the wire. In order to understand these effects on the damage, a numerical model of the spring coiling process has been developed.

The FEM code Simufact.Forming 10.0 is used to perform the 3D mechanical analysis of the coiling process. The wire is fed at the constant velocity of 0.67m/s. A rotation axis in y direction is imposed to the *forming rolls*. Hexahedral elements are adopted to mesh the wire with an element edge size of 2.4mm. The adopted 3D model is shown in Figure 6.

Different combinations of machine setup and friction, which are explained below, have been explored.

Concerning friction condition

- at the interface between wire and the parts of coiling machine where sliding contacts are present (guide, cover plate, pitch bar) the presence/absence of oxide is simulated adopting low/high friction conditions;
- at the interface between wire and rolls low friction condition are always adopted.

Coulomb/Tresca combined law (1-2) was used to model shear stress τ at the interface between the wire and the different parts of tooling system in the coiling machine:

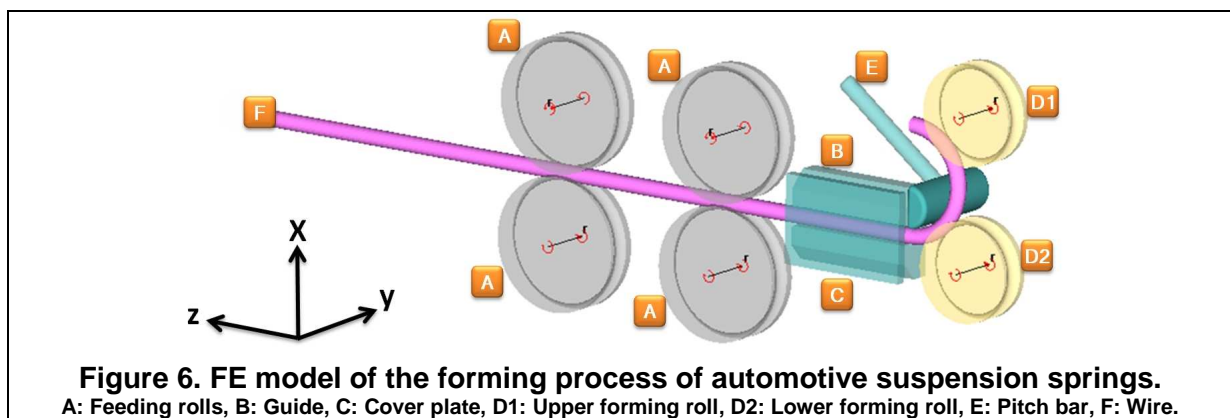
$$\tau = \mu p \quad \text{if} \quad \mu p < \overline{m} \frac{\sigma_0}{\sqrt{3}} \quad (1)$$

$$\tau = \bar{m} \frac{\sigma_0}{\sqrt{3}} \quad \text{if} \quad \mu p > \bar{m} \frac{\sigma_0}{\sqrt{3}} \quad (2)$$

where τ is the friction shear stress, μ (0.03/0.18 for low/high friction coefficient) is the friction coefficient, p is the normal contact pressure at the interface and \bar{m} (0.05/0.3 for low/high friction factor) is the Tresca factor.

Concerning the machine setup

- the variation of coil's diameter (from 85mm to 60mm) is simulated imposing to the upper forming roll a movement in x direction of 29mm;
- the effect of feeding rolls pressure (which is applied in order to avoid slipping of the wire and causes the flattening of the wire) is simulated imposing to the feeders a movement in x direction of 0.5 mm when the wire is prone to slip. This condition is associated to the thinning and breaking of the oxide layer evidenced in the case of the breakage of the coil. When this phenomenon occurs, the steel of the wire is directly in contact with the tooling components and everywhere the wire slides on the tools the friction condition has to be considered at the high value.



4. The material properties

According to the results of tensile tests, the material behaviour can be correctly described by the true stress-true strain curve represented in Figure 7 and derived from the nominal stress-nominal strain curve experimentally recorded (Figure 8). In order to take in account the localized necking developing in the experimental specimen after UTS a numerical model of the tensile test has been used.

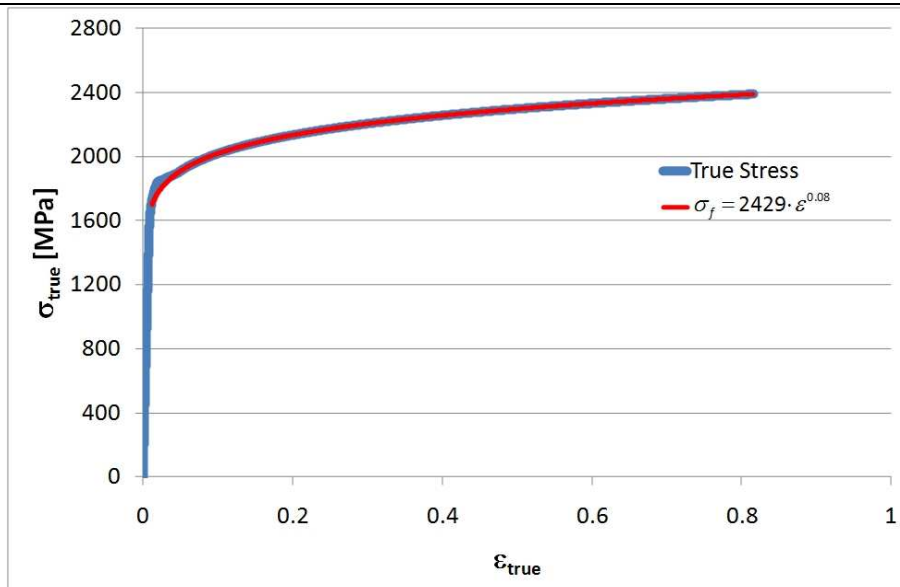


Figure 7. True stress – true strain diagram of the wire.

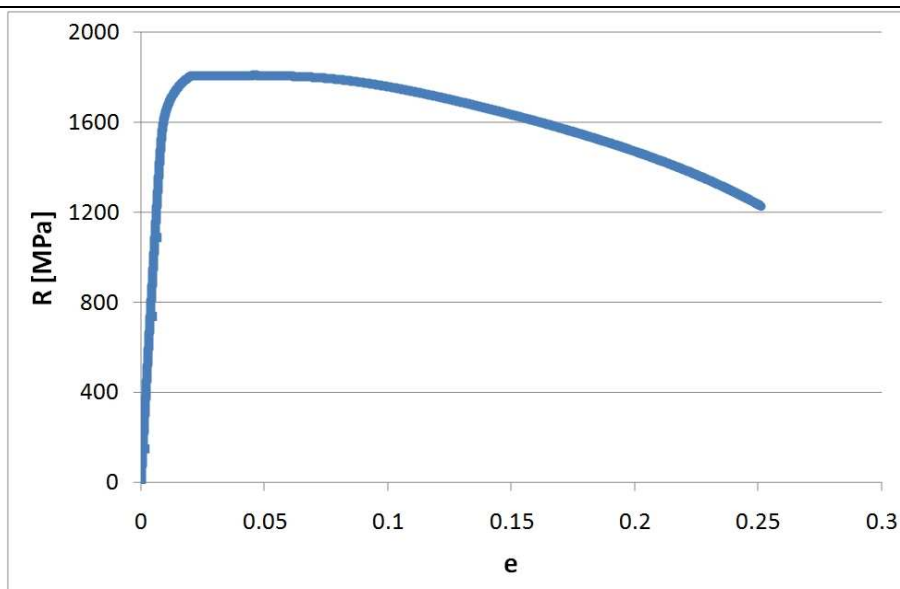


Figure 8. Nominal stress – strain diagram of the wire.

The stress-strain relationship describing the material rheological behaviour has been adjusted in the numerical model of the tensile test until the geometry of the necking zone is reproduced, together with the longitudinal force. The numerical model takes into account for triaxiality of the stresses in the necking zone and for this reason it does not overestimate force and stresses after UTS.

The material has been modelled as elasto plastic with isotropic hardening adopting the power law (3) fitted to the experimental data ($K=2429$ MPa, $n=0.08$).

$$\sigma_f = K \cdot \varepsilon^n \quad (3)$$

where ε is the deformation (total strain), K is the strength coefficient and n is the strain hardening exponent. The elasto-plastic constants of the material are summarized in Table 2.

Basic material constants		Plastic material constants	
Young's Modulus	193 [GPa]	Minimum yield stress	1663 [MPa]
Poisson's ratio	0.28	Yield constant	2429 [MPa]
Density	8027 [kg/m ³]	Strain hardening exponent	0.08

Table 2. Elasto-plastic constants of the material.

The data obtained from tensile test are also used to determine the parameters of the Lemaitre damage model [4] according to the damage mechanics theory of Chaboche and Lemaitre [5].

The damage parameters summarized in Table 3, can be estimated from the experimental data according to the following definitions (4 - 7):

$$D_{1c} = 1 - \frac{R_B}{R_m} \quad (4)$$

$$S = \frac{R_m^2}{2E \frac{D_{1c}}{\varepsilon_B^{pl} - \varepsilon_{R_m}^{pl}}} \quad (5)$$

$$\varepsilon_B^{pl} = 2 \ln \left(\frac{D_0}{D_B} \right) \quad (6)$$

$$\varepsilon_{R_m}^{pl} = \ln(e_{R_m} + 1) - \frac{\sigma_m}{E} \quad (7)$$

where

R_B is is the nominal stress of uniaxial tensile test at the specimen rupture and therefore corrected for triaxiality,

R_m is the nominal stress of uniaxial tensile test at uniform elongation,

ϵ_B^{pl} is the true plastic strain at specimen rupture

$\epsilon_{R_m}^{pl}$ is the true plastic strain at uniform elongation

D_0 is the initial diameter of the specimen

D_B is the minimum diameter of the specimen after rupture

e_{R_m} is the nominal plastic strain at uniform elongation

σ_m is the true stress at the uniform elongation

E is the Young's modulus

The same numerical model of tensile test has been used to get a better estimation of damage parameters of Lemaitre model, specifically the damage resistance S which has been estimated directly from the experimental curve to be between 15 and 18.

Critical damage	0.408
Maximum stress tensile test [MPa]	1810
Damage resistance	16
Equivalent plastic strain at maximum stress	0.035

Table 3. Parameters of the Lemaitre damage model.

5. FEM analysis of spring coiling process

The numerical model previously described has been used to perform numerical simulations of the spring coiling process adopting different friction and process parameters. The relative damage predicted by the software has been used as the index to estimate the risk of failure. The material's undamaged state correspond to relative damage equal to 0 whilst failure is assumed to take place when the relative damage reaches its critical value 1.

FEM analysis of spring with constant diameter of 85 mm

The first FEM analysis was performed in order to simulate the cold forming of a helicoidal spring presenting a constant diameter of the coils (85 mm) and a constant axial pitch (55 mm) in two different process conditions. The first one correspond to the presence of a thick and adherent oxide, the second one simulates the presence of a thin oxide layer broken when the wire is passing between the feeding rolls. This second condition causes slip of the wire and requires to increase the radial pressure of the rolls causing the flattening of the wire.

The results in terms of relative damage for the two process conditions are shown in Figure 9. The maximum relative damage is located at the extrados of the wire and varies from 0.187 to 0.425 respectively. This result confirms that the radial pressure of rolls on the wire introduces a damage on the wire but the level of damage doesn't indicate a risk of failure during the coiling process.

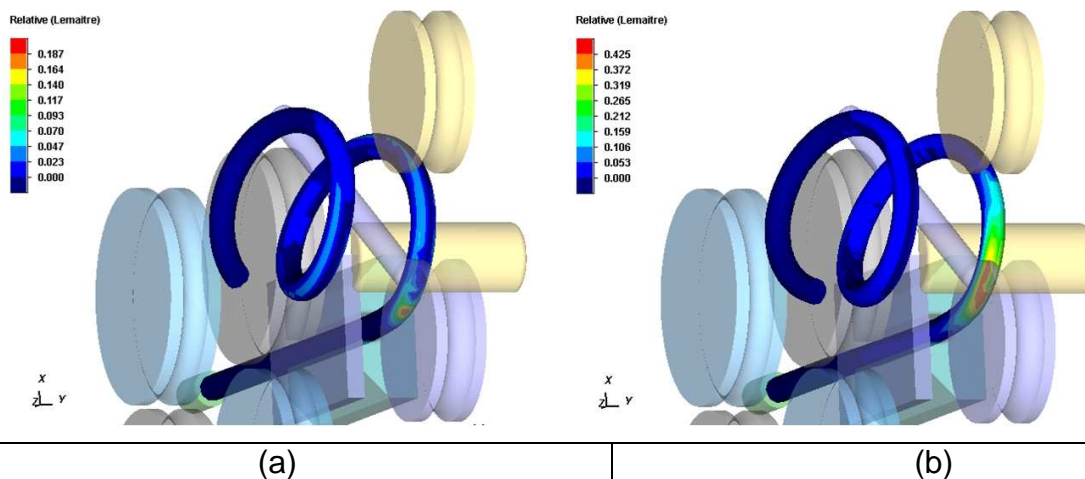
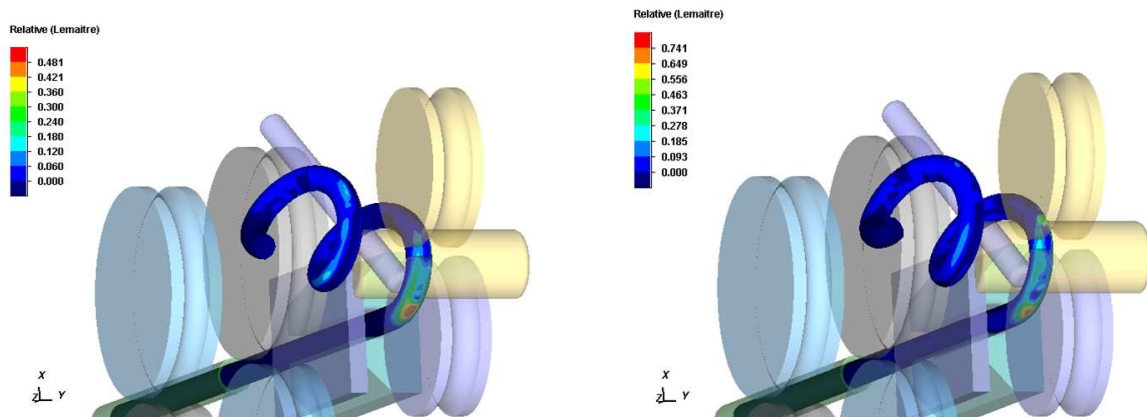


Figure 9. Relative damage in forming of a helicoidal spring with constant diameter of the coils of 85 mm in presence of a thick and adherent oxide (a) and in presence of a thin oxide layer broken when the wire is passing between the feeding rolls (b).

FEM analysis of spring with constant diameter of 60 mm

The second FEM analysis was performed to simulate the cold forming of a helicoidal spring presenting a constant diameter of the coils (60 mm) and a constant axial pitch (55 mm) in the same process conditions described in the previous case. The bending of the wire for the 60 mm coil is higher than the bending for the 85 mm coil and higher values of damage should be expected.

The relative damages predicted by the software for the two process conditions are shown in Figure 10. As in the previous case, the maximum relative damage is located at the extrados of the wire and varies from 0.481 to 0.741, confirming that the damage level is higher respect to the case of forming wire with a diameter of 85 mm. However, even in this case, the level of damage doesn't indicate a risk of failure during the coiling process.



(a)	(b)
Figure 10. Relative damage in forming of a helicoidal spring with constant diameter of the coils of 60 mm in presence of a thick and adherent oxide (a) and in presence of a thin oxide layer broken when the wire is passing between the feeding rolls (b).	

FEM analysis of spring with varying diameter from 85 mm to 60 mm

The third FEM analysis simulates the cold forming of a helicoidal spring with a varying diameter between 85 mm and 60 mm and a varying axial pitch between 55 mm and 32 mm in the same conditions of the previous cases.

The relative damages for the two process conditions are shown in Figure 11. The maximum relative damage is at the extrados of the wire and, depending on process conditions, varies from 0.488 to 0.973. In the case of high pressure of feeding rolls, the damage level (0.973) is higher respect to the previous cases indicating a risk of failure during the coiling process. Therefore it is possible to conclude that the variation of diameter and axial pitch together with the presence of thin and not adherent oxide layer can lead to failure during coiling of the wire. This result is confirmed analyzing the cracked springs. The fracture is located in the zone where variation of diameter takes place.

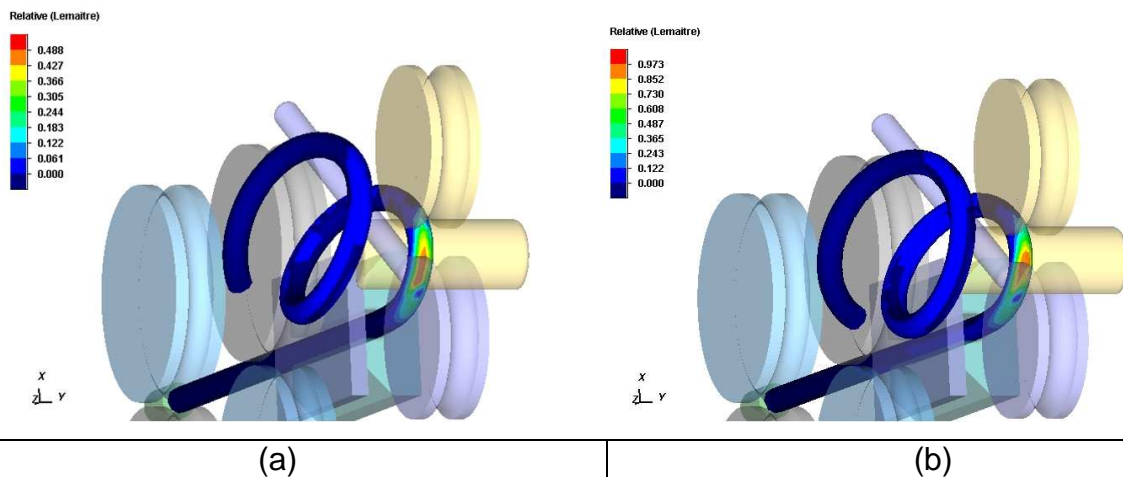


Figure 11. Relative damage in forming of a helicoidal spring with varying diameter between 85 mm and 60 mm in presence of a thick and adherent oxide (a) and in presence of a thin oxide layer broken when the wire is passing between the feeding rolls (b).

6. Conclusions

Spring manufacturing by cold forming of pre hardened steel is critical when the material ultimate tensile strength is above 1800 MPa. The quality and the thickness of the oxide layer on the external surface of the wire affect the success/failure of the coiling process as the oxide acts as a sort of solid lubricant and its removal leads to an increase of friction phenomena. The higher friction forces increase both the required forming force and the feeding force, which can introduce some damages in the wire and finally can cause the breakage of the coil.

The numerical model developed for the coiling process can take in account such effects and the implementation of ductile isotropic damage based on Lemaitre formulation allows the correct prediction of the failure during coiling. The extensive utilization of the model permits to explore different interactions between machine setup and friction, determining the configuration that should be adopted to avoid the risk of failure.

7. References

- [1] Prawoto, Y., Ikeda, M., Manville, S.K., Nishikawa, A.: Design and failure modes of automotive suspension springs. *Engineering failure analysis*, 15 (2008) 20. 1155 - 1174.
- [2] Ardehali Barani, A., Li, F., Romano, P., Ponge, D., Raabe, D.: Design of high-strength steels by microalloying and thermomechanical treatment. *Materials Science and Engineering*, 463 (2007) 9. 138 - 146.
- [3] Wise, J.P., Spice, J., Davidson, S.G., Heitmann, W.E., Krauss, G.: Influence of short austenitizing times on the fracture behavior of a microalloyed automotive spring steel. *Scripta mater.*, 44 (2001). 299 - 304.
- [4] Simufact Technical References: Crack prediction in massive forming via simulation, 2009.
- [5] Lemaitre, J., Chaboche, J. L.: *Mechanics of Solid Materials*. Cambridge University Press, 1990.

University of Padua, DTG
Stradella San Nicola, 3
36100 Vicenza (Italy)
Tel.: +39 0444 998724
Fax: +39 0444 998889
e-mail: guido.ber ti@unipd.it or manuel.monti@unipd.it
www.unipd.it

